

# Phase Diagrams of the Ternary Systems $\text{NaBH}_4 + \text{NaOH} + \text{H}_2\text{O}$ , $\text{KBH}_4 + \text{KOH} + \text{H}_2\text{O}$ , $\text{NaBO}_2 + \text{NaOH} + \text{H}_2\text{O}$ , and $\text{KBO}_2 + \text{KOH} + \text{H}_2\text{O}$ at $-10\text{ }^\circ\text{C}$

Alexei V. Churikov,\* Konstantin V. Zapsis, Victor V. Khrankov, Mikhail A. Churikov, Maksim P. Smotrov, and Ivan A. Kazarinov

Institute of Chemistry, Saratov State University, 83 Astrakhanskaya Str., Saratov 410012, Russian Federation

Concentrated water–alkaline solutions of sodium and potassium borohydrides are used as a fuel and as a hydrogen source in hydrogen power engineering, including low-temperature fuel cells, where borohydrides are converted into metaborates. The performance of such mixtures is determined by the solubility of their components, negative temperatures being especially critical. The solubility in the ternary systems  $\text{NaBH}_4 + \text{NaOH} + \text{H}_2\text{O}$ ,  $\text{KBH}_4 + \text{KOH} + \text{H}_2\text{O}$ ,  $\text{NaBO}_2 + \text{NaOH} + \text{H}_2\text{O}$ , and  $\text{KBO}_2 + \text{KOH} + \text{H}_2\text{O}$  was studied by means of isothermal saturation at  $-10\text{ }^\circ\text{C}$ . The compositions of the equilibrium solid phases and of mixtures corresponding to nonvariant equilibrium points were determined; the solubility diagrams of the systems were plotted. The presence of a range of homogeneous solutions and fields of crystallization of ice, anhydrous, and hydrated forms of the salts and hydroxides is characteristic of all four systems at the said temperature. The composition of crystalline hydrates depends on the ratio of the components in the mixture and on the cation nature. Of the borohydride systems, the best solubility was observed in that with  $\text{NaBH}_4$ , whereas in the metaborate systems it was that with  $\text{KBO}_2$ .

## Introduction

Nowadays, much research in hydrogen power engineering and chemical power sources is devoted to the development of novel fuel cells (FCs).<sup>1–4</sup> One of the promising directions of research involves low-temperature FCs, in which salt-like borohydrides of alkaline metals,  $(\text{Na}, \text{K})\text{BH}_4$ , are used as a source of hydrogen (fuel). From their characteristics, they are comparable with methanol-utilizing FCs.<sup>4</sup> In such devices, borohydrides are used in the form of suspensions or concentrated aqueous solutions with dissolved hydroxides,  $(\text{Na}, \text{K})\text{OH}$ , as additives which stabilize the system by preventing borohydride ion  $(\text{BH}_4^-)$  hydrolysis as well as determining and controlling its chemical and electrochemical activity. During FC functioning, borohydrides are oxidized, releasing the contained hydrogen and being converted into soluble salts of boric acid, that is, metaborates,  $(\text{Na}, \text{K})\text{BO}_2$ .

Thus, the initial fuel belongs by its composition to the ternary systems  $\text{NaBH}_4 + \text{NaOH} + \text{H}_2\text{O}$  or  $\text{KBH}_4 + \text{KOH} + \text{H}_2\text{O}$ , while the final product to the ternary systems  $\text{NaOH} + \text{NaBO}_2 + \text{H}_2\text{O}$  or  $\text{KOH} + \text{KBO}_2 + \text{H}_2\text{O}$ . There are reports devoted to studying the aqueous solubility of  $\text{NaOH}$ ,  $\text{NaBO}_2$ ,  $\text{NaBH}_4$ ,  $\text{KOH}$ ,  $\text{KBH}_4$ , and  $\text{KBO}_2$  both as individual substances and in various combinations. Some earlier papers dealt with the solubility polytherms of the binary alkaline systems  $\text{NaOH} + \text{H}_2\text{O}$ <sup>5,6</sup> and  $\text{KOH} + \text{H}_2\text{O}$ ;<sup>7</sup> information is also available on the binary systems  $\text{NaBH}_4 + \text{H}_2\text{O}$ ,<sup>6</sup>  $\text{KBH}_4 + \text{H}_2\text{O}$ ,<sup>7</sup>  $\text{NaBO}_2 + \text{H}_2\text{O}$ , and  $\text{KBO}_2 + \text{H}_2\text{O}$ .<sup>8–10</sup>

Some information on the ternary-system solubility diagrams under consideration is presented in refs 6 to 8, 11, and 12. In ref 11, the solubility isotherms of the purely alkaline ternary system  $\text{NaOH} + \text{KOH} + \text{H}_2\text{O}$  were studied within a temperature range of  $(0\text{ to }20)\text{ }^\circ\text{C}$ . Crystalline hydrates were shown to be in

equilibrium with the solution, while anhydrous  $\text{NaOH}$  and  $\text{KOH}$  existed only under water deficiency (mixtures with mass fractions of alkali  $w > 0.75$ ). The isotherms of the ternary systems  $\text{NaBH}_4 + \text{NaOH} + \text{H}_2\text{O}$  and  $\text{KBH}_4 + \text{KOH} + \text{H}_2\text{O}$  within  $(0\text{ to }50)\text{ }^\circ\text{C}$  were investigated by Mikheyeva et al.<sup>6,7,12</sup> and also in ref 13. Some general regularities of the behavior of those systems were noted; in particular, alkali and borohydride were shown to lower the solubility of each other, but the total concentration of the saturated solution increased. Solid phases exist as crystalline hydrates of various compositions. Increasing the temperature is accompanied by growth of the solubility of all solid phases, the solubility of borohydride increasing more rapidly than that of the alkali. Simultaneously, dehydration of crystalline hydrates occurs with the appearance and growth of an anhydrous salt field, so that at  $50\text{ }^\circ\text{C}$  the solid phases are represented by the anhydrous compounds  $\text{NaBH}_4$ ,  $\text{NaOH}$ ,  $\text{KBH}_4$ , and  $\text{KOH}$ .

It can be seen that the early studies have been performed within the temperature range from  $(0\text{ to }50)\text{ }^\circ\text{C}$ , whereas the expected functionality of borohydride FCs covers the range below  $0\text{ }^\circ\text{C}$  as well. The performance of fuel mixtures are determined by concentrations of the dissolved components, negative temperatures being especially critical. Decreasing temperature may result in the formation of additional solid phases, a solubility decrease, and shrinkage of the homogeneous liquid state field. No literature data have been found on the solubilities in the ternary systems  $\text{NaOH} + \text{NaBO}_2 + \text{H}_2\text{O}$  and  $\text{KOH} + \text{KBO}_2 + \text{H}_2\text{O}$ .

Therefore, studying the aforementioned systems to obtain more complete information about the character of component solubility in the alkali + borohydride + water and alkali + metaborate + water mixtures is of both fundamental and practical importance. In the present work, the ternary systems  $\text{NaBH}_4 + \text{NaOH} + \text{H}_2\text{O}$ ,  $\text{KBH}_4 + \text{KOH} + \text{H}_2\text{O}$ ,  $\text{NaOH} + \text{NaBO}_2 + \text{H}_2\text{O}$ , and  $\text{KOH} + \text{KBO}_2 + \text{H}_2\text{O}$  have been studied

\* Corresponding author. Tel.: +7-8452-516413. Fax: +7-8452-271491. E-mail address: churikovav@inbox.ru.

by means of isothermal saturation at  $-10\text{ }^{\circ}\text{C}$ . For these systems, the compositions of the solid phases and mixtures corresponding to nonvariant equilibrium points have been determined and solubility isotherms plotted on the composition triangles, and the results obtained are analyzed and compared with the relevant literature data.

### Experimental Section

Solubilities were measured in special glass vessels with a mechanical stirrer, glycerol seal to prevent gas exchange with the atmosphere, and a thermostatted sampling tube.<sup>14</sup> The composition of the loaded mixture was calculated considering the crystallization water in the reagents. The following chemicals ("reagent grade" quality) were used:  $\text{NaBO}_2 \cdot 4\text{H}_2\text{O}$  and  $\text{KBO}_2 \cdot 1.25\text{H}_2\text{O}$  (Vekton, Russian Federation);  $\text{NaOH}$  and  $\text{KOH}$  (ECROS, Russian Federation);  $\text{NaBH}_4$  and  $\text{KBH}_4$  (Aviabor, Russian Federation); distilled water with no dissolved carbon dioxide. The amount of the loaded mixture was (35 to 40) g per experiment; weighing with an uncertainty of  $\pm 1$  mg was carried out with a VLT 150P laboratory electronic balance. The saturation of solutions was performed in a PolySciens "Al-exRedCTD" programmed thermostat at a fixed temperature [ $-10 \pm 0.01$ ]  $^{\circ}\text{C}$ .

After filling the vessel with the mixture studied, it was thermostatted under continuous stirring. The equilibration time in each system was estimated by sampling the saturated solution and analyzing its chemical composition. Equilibrium was established in ca. (2 to 3) h of stirring. After mixture settling, three samples of the saturated solution and two to three samples of the precipitate were taken. The sampling of the liquid was implemented by its replacement through a cotton wool filter. For sampling the solid phase, the saturated suspension was displaced, which then was filtered through a Schott glass filter under vacuum, separating the precipitate from the mother liquor and then pressing it between sheets of filter paper. The fact that the precipitate inevitably contained some mother liquor was insignificant, since the composition of the solid phase was determined by Schreinemakers' method. In this method, the straight line drawn through the compositions of the liquid phase and the corresponding wet solids passes through the composition of the pure solid phase on the phase diagram; thus, the composition of the pure solid phase is obtained from the intersection of lines drawn through several such pairs.

The composition of the saturated solution and the solid phase was determined by quantitative chemical analysis. For the systems containing a mixture of alkali and borate, an acid–base titration was employed. For this purpose, a sample of liquid solution of (0.2 to 0.5) g or that of precipitate of (0.3 to 0.6) g was quantitatively transferred to a glass for titration, with further diluting with distilled water up to 50 mL. The titration was done with a  $1\text{ mol}\cdot\text{L}^{-1}$   $\text{HCl}$  solution. Titration curves (Figure 1a) were processed by computer fitting of experimental and calculated titration curves.

The compositions of the equilibrium phases in the systems containing alkali and borohydride were analyzed by means of two different techniques. The alkali content was determined by acid–base titration. For borohydride analysis, an iodometric titration was used (Figure 1b). A liquid sample [(0.2 to 0.5) g] or that of the precipitate [(0.3 to 0.6) g] was quantitatively transferred to a 100 mL flask and brought to the mark with a  $1\text{ mol}\cdot\text{L}^{-1}$   $\text{NaOH}$  solution. Then, a 5 mL aliquot was sampled, transferred to a glass for titration, and brought to 50 mL with a  $1\text{ mol}\cdot\text{L}^{-1}$   $\text{NaOH}$  solution with further titration using a  $0.1\text{ mol}\cdot\text{L}^{-1}$  standard iodine solution.

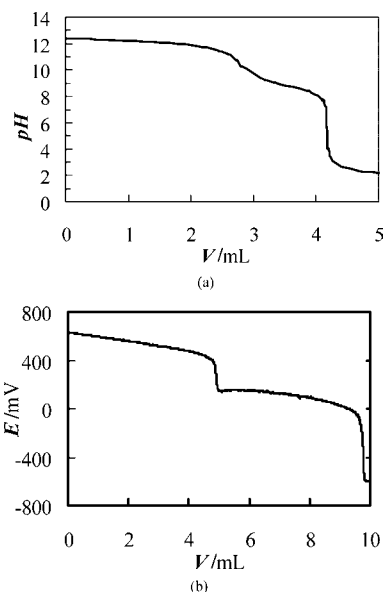


**Figure 1.** Typical curves of (a) acid–base titration and (b) iodometric titration of the solutions under study. Consecutive titrating steps correspond to (a) the titration of the hydroxide ion and the borate ion or to (b) the complex mechanism of the interaction  $\text{I}_2 + \text{BH}_4^-$ .

**Table 1.** Equilibrium Data for the  $\text{NaBH}_4 + \text{NaOH} + \text{H}_2\text{O}$  System at  $-10\text{ }^{\circ}\text{C}^a$

composition of liquid phase (100 w)			composition of wet solid phase (100 w)			equilibrium crystalline phases
$\text{NaBH}_4$	$\text{NaOH}$	$\text{H}_2\text{O}$	$\text{NaBH}_4$	$\text{NaOH}$	$\text{H}_2\text{O}$	
23.4	0.0	76.6				$\text{NaBH}_4 \cdot 2\text{H}_2\text{O}$
18.9	0.0	81.1				ice
<u>18.3</u>	<u>27.3</u>	<u>54.4</u>	<u>51.3</u>	<u>7.7</u>	<u>41.0</u>	$\text{NaBH}_4 + \text{NaBH}_4 \cdot 2\text{H}_2\text{O}$ ( <i>p1</i> )
17.0	23.1	59.9	38.2	6.9	54.9	ice
16.1	8.2	75.7	42.3	4.6	53.1	$\text{NaBH}_4 \cdot 2\text{H}_2\text{O}$
14.6	32.7	52.7	82.2	7.0	10.8	$\text{NaBH}_4$
14.4	14.1	71.5	38.6	6.3	55.1	$\text{NaBH}_4 \cdot 2\text{H}_2\text{O}$
14.0	18.5	67.5	42.1	3.8	54.1	$\text{NaBH}_4 \cdot 2\text{H}_2\text{O}$
13.8	4.4	81.8	11.7	3.7	84.6	ice
12.2	38.2	49.6	74.5	10.6	14.9	$\text{NaBH}_4$
<u>10.5</u>	<u>42.6</u>	<u>46.9</u>	<u>12.6</u>	<u>54.0</u>	<u>33.4</u>	$\text{NaBH}_4 + \text{NaOH} \cdot \text{H}_2\text{O}$ ( <i>e1</i> )
9.3	37.1	53.6	3.2	55.9	40.9	$\text{NaOH} \cdot \text{H}_2\text{O}$
8.3	33.5	58.2	1.8	60.1	38.1	$\text{NaOH} \cdot \text{H}_2\text{O}$
7.6	8.4	84.0	6.7	7.2	86.1	ice
6.2	31.3	62.5	2.6	52.6	44.8	$\text{NaOH} \cdot \text{H}_2\text{O}$
<u>3.2</u>	<u>29.6</u>	<u>67.2</u>	<u>1.7</u>	<u>41.8</u>	<u>56.5</u>	$\text{NaOH} \cdot \text{H}_2\text{O} + \text{NaOH} \cdot 4\text{H}_2\text{O}$ ( <i>p2</i> )
2.6	10.6	86.8	1.7	6.7	91.6	ice
1.6	26.4	72.0	0.9	31.1	68.0	$\text{NaOH} \cdot 4\text{H}_2\text{O}$
0.0	26.7	73.3				$\text{NaOH} \cdot 4\text{H}_2\text{O}$
0.0	9.8	90.2				ice

<sup>a</sup> Compositions and the equilibrium crystalline phases of peritonic points (*p1*, *p2*) and eutonic point (*e1*) are underlined.

The results of our experiments are presented as Gibbs–Roseboom triangles, the vertices of which correspond to pure components, the points on the sides to the compositions of the binary systems, and the points inside the triangles characterize the compositions of ternary mixtures. For each system under study, no less than 20 points were obtained; the liquidus lines and crystallization fields of solid phases were determined.

### Results and Discussion

The results of the determination of the solubility and composition of equilibrium solid phases in the  $\text{NaBH}_4 + \text{NaOH} + \text{H}_2\text{O}$  system are presented in Table 1 and Figure 2. The area of liquid phase *l* is limited by the crystallization lines of five solid phases. One of them cuts off the ice crystallization area adjacent to the  $\text{H}_2\text{O}$  vertex; the others limit the crystallization areas of alkali and metaborate.

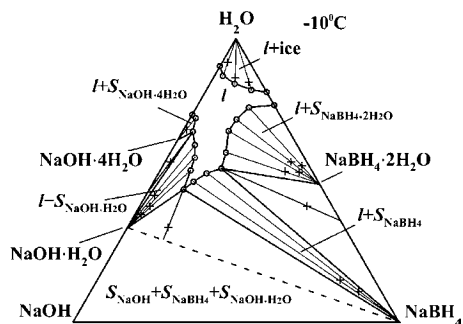


**Figure 2.** Phase diagram for the  $\text{NaBH}_4 + \text{NaOH} + \text{H}_2\text{O}$  system at  $-10$  °C.  $l$  and  $S$  are liquid and solid phases, respectively. Compositions of the equilibrium liquid phase ( $\circ$ ) and wet solid phase ( $+$ ) are listed in Table 1. Thin lines are tie-lines between coexisting phases, and thick solid and dashed lines are the bounds among monophasic, two-phase, and three-phase areas.

Let us analyze the course of solubility and phase ratios, considering the diagram from the right to the left. The range of homogeneous liquid solution in the  $\text{NaBH}_4 + \text{H}_2\text{O}$  system is  $w = (0.189 \text{ to } 0.234)$  at  $-10$  °C. Solutions with lower  $\text{NaBH}_4$  concentrations contain ice crystals. Increasing the borohydride concentration results in the onset of the equilibrium “liquid + solid  $\text{NaBH}_4 \cdot 2\text{H}_2\text{O}$ ” in the system. Our data agree well with the results of earlier work,<sup>6</sup> except for the borders of the homogeneous solution in the binary  $\text{NaBH}_4 + \text{H}_2\text{O}$  system. According to ref 6, a homogeneous liquid solution at  $-10$  °C exists at  $\text{NaBH}_4$  fractions  $w \approx (0.09 \text{ to } 0.26)$ .

The ice crystallization range ( $l + \text{ice}$ ) is located at the water vertex of the triangle. This area is cut off by the upper liquidus line, connecting the triangle’s sides at mass fractions of 0.189 for borohydride and 0.106 for alkali. The liquid solution  $l$  area is limited by the lower liquidus line, consisting of four sections connected by one eutonic point  $e1$  and two peritonic points  $p1$  and  $p2$ ; their compositions are given in Table 1. The eutonic  $l + S_{\text{NaBH}_4} + S_{\text{NaOH} \cdot \text{H}_2\text{O}}$  triangle is characterized by equilibrium between the phases of the saturated solution, anhydrous borohydride, and alkali monohydrate. On the right side of the eutonic triangle there are two borohydride crystallization fields corresponding to the anhydrous salt ( $l + S_{\text{NaBH}_4}$ ) and monohydrate ( $l + S_{\text{NaBH}_4 \cdot 2\text{H}_2\text{O}}$ ).

On the left of the eutonic triangle there are alkali crystallization fields. In the  $l + S_{\text{NaOH} \cdot \text{H}_2\text{O}}$  area there exists  $\text{NaOH} \cdot \text{H}_2\text{O}$ , the  $l + S_{\text{NaOH} \cdot 4\text{H}_2\text{O}}$  range corresponds to  $\text{NaOH} \cdot 4\text{H}_2\text{O}$ , and the presence of the latter is characteristic of this system. References 6 and 15 to 17 have revealed no existence of the tetrahydrate  $\text{NaOH} \cdot 4\text{H}_2\text{O}$  in the  $\text{NaBH}_4 + \text{NaOH} + \text{H}_2\text{O}$  system within (0 to 50) °C. This tetrahydrate, according to the  $\text{NaOH} + \text{H}_2\text{O}$  solubility polytherms,<sup>5</sup> crystallizes at negative temperatures and alkali fractions within (0.25 to 0.35). Three-phase peritonic equilibria correspond to the  $\text{NaBH}_4 \cdot 2\text{H}_2\text{O} \leftrightarrow \text{NaBH}_4$  ( $p1$ ) and  $\text{NaOH} \cdot 4\text{H}_2\text{O} \leftrightarrow \text{NaOH} \cdot \text{H}_2\text{O}$  ( $p2$ ) transitions. The solid  $\text{NaOH} + \text{NaOH} \cdot \text{H}_2\text{O} + \text{NaBH}_4$  mixture exists at the bottom part of the diagram.

Analyzing the mutual component solubility in a similar potassium system, the solubility data are given in Table 2 and Figure 3. First, note an essentially lower solubility of potassium borohydride as compared with that of sodium borohydride, which is extremely important from a practical viewpoint. The maximum  $\text{KBH}_4$  solubility at  $-10$  °C is  $w = 0.113$  ( $e2$  point); it is reached in pure water (this value agrees well with the polythermal data of the binary  $\text{KBH}_4 + \text{H}_2\text{O}$  system<sup>7</sup>). The introduction of alkali into the system sharply reduces the  $\text{KBH}_4$  solubility, which falls down to  $w < 0.01$  in concentrated alkaline

**Table 2.** Equilibrium Data for the  $\text{KBH}_4 + \text{KOH} + \text{H}_2\text{O}$  System at  $-10$  °C<sup>a</sup>

composition of liquid phase (100 w)			composition of wet solid phase (100 w)			equilibrium crystalline phases
$\text{KBH}_4$	$\text{KOH}$	$\text{H}_2\text{O}$	$\text{KBH}_4$	$\text{KOH}$	$\text{H}_2\text{O}$	
11.3	0.0	88.7				ice + $\text{KBH}_4 \cdot 3\text{H}_2\text{O}$ ( $e2$ )
11.1	0.7	88.2	29.2	0.3	70.5	$\text{KBH}_4 \cdot 3\text{H}_2\text{O}$
10.6	2.1	87.3	34.7	1.2	64.1	$\text{KBH}_4 \cdot 3\text{H}_2\text{O} + \text{KBH}_4 \cdot \text{H}_2\text{O}$ ( $p3$ )
9.5	1.8	88.7	6.5	1.2	92.3	ice
9.1	3.5	87.4	58.7	1.1	40.2	$\text{KBH}_4 \cdot \text{H}_2\text{O}$
7.6	5.8	86.6	53.7	2.2	44.1	$\text{KBH}_4 \cdot \text{H}_2\text{O}$
6.1	5.8	88.1	5.0	4.5	90.5	ice
5.3	9.3	85.4	45.4	7.2	47.4	$\text{KBH}_4 \cdot \text{H}_2\text{O}$
3.1	14.9	82.0	31.1	7.4	61.5	$\text{KBH}_4 \cdot \text{H}_2\text{O}$
3.0	12.9	84.1	38.3	9.1	52.6	$\text{KBH}_4 \cdot \text{H}_2\text{O}$
1.7	11.3	87.0	1.1	6.3	92.6	ice
1.6	21.0	77.4	47.8	7.2	45.0	$\text{KBH}_4 \cdot \text{H}_2\text{O}$
0.8	44.1	55.1	53.9	12.5	33.6	$\text{KBH}_4 \cdot \text{H}_2\text{O}$
0.8	34.4	64.8	45.5	13.5	41.0	$\text{KBH}_4 \cdot \text{H}_2\text{O}$
0.7	11.7	87.6	43.5	11.3	45.2	$\text{KBH}_4 \cdot \text{H}_2\text{O}$
0.7	48.0	51.3	8.8	46.8	44.4	$\text{KOH} \cdot \text{H}_2\text{O} + \text{KBH}_4 \cdot \text{H}_2\text{O}$ ( $e3$ )
0.6	38.1	61.3	42.5	16.5	41.0	$\text{KBH}_4 \cdot \text{H}_2\text{O}$
0.2	47.0	52.8				$\text{KOH} \cdot \text{H}_2\text{O}$
0.0	48.8	51.2				$\text{KOH} \cdot \text{H}_2\text{O}$
0.0	12.1	87.9				ice

<sup>a</sup> Compositions and the equilibrium crystalline phases of peritonic point ( $p3$ ) and eutonic points ( $e2$ ,  $e3$ ) are underlined.

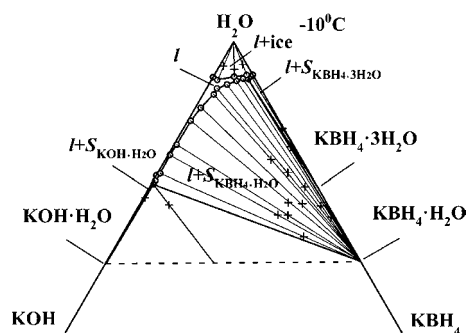


**Figure 3.** Phase diagram for the  $\text{KBH}_4 + \text{KOH} + \text{H}_2\text{O}$  system at  $-10$  °C.  $l$  and  $S$  are liquid and solid phases, respectively. Compositions of the saturated liquid solution ( $\circ$ ) and wet solid phase ( $+$ ) are listed in Table 2. Thin lines are tie-lines between coexisting phases, and thick solid and dashed lines are the bounds among monophasic, two-phase, and three-phase areas.

solutions. Therefore, the major part of the triangle’s area is occupied by the crystallization fields of  $\text{KOH}$ ,  $\text{KBH}_4$ , and their hydrates. The main field corresponds to the crystallization of monohydrate  $l + S_{\text{KBH}_4 \cdot \text{H}_2\text{O}}$ . Below is the eutonic  $l + S_{\text{KBH}_4 \cdot \text{H}_2\text{O}} + S_{\text{KOH} \cdot \text{H}_2\text{O}}$  triangle; the eutonic solution  $e3$  is mainly formed by  $\text{KOH}$ . In the water vertex of the diagram, an ice crystallization field ( $l + \text{ice}$ ) is located. The peritonic point  $p3$  ( $l + S_{\text{KBH}_4 \cdot 3\text{H}_2\text{O}} + S_{\text{KBH}_4 \cdot \text{H}_2\text{O}}$  equilibrium) can only be found with difficulty.

The phase diagram  $\text{KBH}_4 + \text{KOH} + \text{H}_2\text{O}$  also contains two very narrow heterogeneous fields, namely: (i) that of trihydrate  $\text{KBH}_4 \cdot 3\text{H}_2\text{O}$  crystallization, the  $l + S_{\text{KBH}_4 \cdot 3\text{H}_2\text{O}}$  field adjoining the borohydride side of the diagram; (ii) that of monohydrate  $\text{KOH} \cdot \text{H}_2\text{O}$  crystallization, the  $l + S_{\text{KOH} \cdot \text{H}_2\text{O}}$  field adjoining the alkali side. The trapezoid region at the bottom of the diagram corresponds to the existence of a solid mixture of anhydrous components and their crystalline hydrates. However, we did not investigate the region of solid mixtures; therefore, phase equilibria are not shown.

As was noted above, there is little solubility data in the literature for the binary systems metaborate + water and no systematic reports on the ternary systems alkali + metaborate

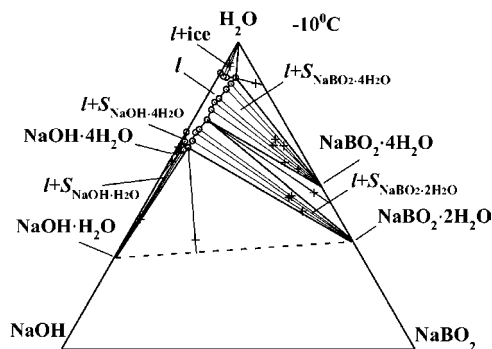


**Figure 4.** Phase diagram for the  $\text{NaBO}_2 + \text{NaOH} + \text{H}_2\text{O}$  system at  $-10^\circ\text{C}$ .  $l$  and  $S$  are liquid and solid phases, respectively. Compositions of the saturated liquid solution ( $\circ$ ) and wet solid phase ( $+$ ) are listed in Table 3. Thin lines are tie-lines between coexisting phases, and thick solid and dashed lines are the bounds among monophasic, two-phase, and three-phase areas.

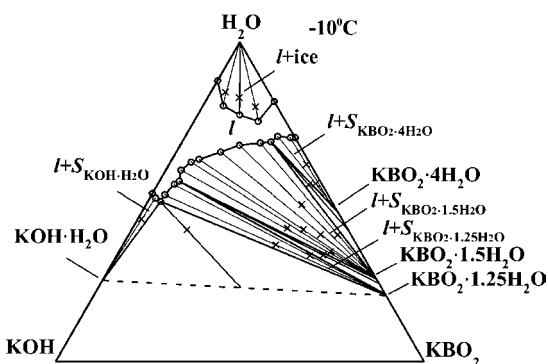


**Figure 5.** Phase diagram for the  $\text{KBO}_2 + \text{KOH} + \text{H}_2\text{O}$  system at  $-10^\circ\text{C}$ .  $l$  and  $S$  are liquid and solid phases, respectively. Compositions of the saturated liquid solution ( $\circ$ ) and wet solid phase ( $+$ ) are listed in Table 4. Thin lines are tie-lines between coexisting phases, and thick solid and dashed lines are the bounds among monophasic, two-phase, and three-phase areas.

+ water. For instance, in refs 8 to 10, the solubility polytherms of the  $\text{NaBO}_2 + \text{H}_2\text{O}$  and  $\text{KBO}_2 + \text{H}_2\text{O}$  systems were studied in different temperature ranges. It has been shown that the eutectic in the  $\text{KBO}_2 + \text{H}_2\text{O}$  system lies at  $-20^\circ\text{C}$ , and a homogeneous solution exists within  $w \approx (0.24 \text{ to } 0.32)$  of  $\text{KBO}_2$  at  $-10^\circ\text{C}$ .<sup>10</sup> The system  $\text{NaBO}_2 + \text{H}_2\text{O}$  has not been studied at  $-10^\circ\text{C}$ .

Figures 4 and 5 show the isothermal phase diagrams of the ternary borate + alkali systems, and Tables 3 and 4 contain the coordinates of the experimental points. The diagram of the  $\text{NaBO}_2 + \text{NaOH} + \text{H}_2\text{O}$  system at  $-10^\circ\text{C}$  is rather complex (Figure 4) and is characterized by the presence of two eutonic points  $e4$  and  $e5$ , two peritonic points  $p4$  and  $p5$ , and five crystallization fields. The crystallization fields of ice ( $l + \text{ice}$ ) and  $\text{NaBO}_2 \cdot 4\text{H}_2\text{O}$  ( $l + S_{\text{NaBO}_2 \cdot 4\text{H}_2\text{O}}$ ) adjoin the eutonic triangle with vertex  $e4$ , while fields  $l + S_{\text{NaBO}_2 \cdot 2\text{H}_2\text{O}}$  and  $l + S_{\text{NaOH} \cdot \text{H}_2\text{O}}$  adjoin the eutonic triangle with vertex  $e5$ . The solubility of sodium metaborate is low and generally decreases with increasing  $\text{NaOH}$  content, while the total solubility grows.

The tetrahydrate  $\text{NaBO}_2 \cdot 4\text{H}_2\text{O}$  precipitates at low alkali contents and loses crystallization water with increasing  $\text{NaOH}$  concentration in the system, resulting in the formation of the  $\text{NaBO}_2 \cdot 4\text{H}_2\text{O} + \text{NaBO}_2 \cdot 2\text{H}_2\text{O}$  peritonic point  $p4$ . As to the  $\text{NaOH}$  crystallization field, the peritonic decomposition at increasing alkalinity of the system occurs as well:  $\text{NaOH} \cdot 4\text{H}_2\text{O}$  decomposes into  $\text{NaOH} \cdot \text{H}_2\text{O}$  and water. The bottom part of the diagram corresponds to a mixture of solid components.

**Table 3.** Equilibrium Data for the  $\text{NaBO}_2 + \text{NaOH} + \text{H}_2\text{O}$  System at  $-10^\circ\text{C}^a$

composition of liquid phase (100 w)			composition of wet solid phase (100 w)			equilibrium crystalline phases
$\text{NaBO}_2$	$\text{NaOH}$	$\text{H}_2\text{O}$	$\text{NaBO}_2$	$\text{NaOH}$	$\text{H}_2\text{O}$	
5.1	6.6	88.3	11.7	1.8	86.5	ice + $\text{NaBO}_2 \cdot 4\text{H}_2\text{O}$ ( $e4$ )
4.8	8.9	86.3	29.8	4.1	66.1	$\text{NaBO}_2 \cdot 4\text{H}_2\text{O}$
4.3	11.1	84.6	26.3	5.4	68.3	$\text{NaBO}_2 \cdot 4\text{H}_2\text{O}$
3.8	21.5	74.7	46.3	3.0	50.7	$\text{NaBO}_2 \cdot 2\text{H}_2\text{O} + \text{NaBO}_2 \cdot 4\text{H}_2\text{O}$ ( $p4$ )
3.8	14.7	81.5	26.7	7.0	66.3	$\text{NaBO}_2 \cdot 4\text{H}_2\text{O}$
3.5	18.6	77.9	32.8	6.4	60.8	$\text{NaBO}_2 \cdot 4\text{H}_2\text{O}$
3.2	25.2	71.6	40.1	10.1	49.8	$\text{NaBO}_2 \cdot 2\text{H}_2\text{O}$
3.1	29.1	67.8	45.6	9.4	45.0	$\text{NaBO}_2 \cdot 2\text{H}_2\text{O}$
3.1	16.5	80.4	37.6	3.7	58.7	$\text{NaBO}_2 \cdot 4\text{H}_2\text{O}$
3.0	31.4	65.6	20.2	44.3	35.5	$\text{NaOH} \cdot \text{H}_2\text{O} + \text{NaBO}_2 \cdot 2\text{H}_2\text{O}$ ( $e5$ )
2.7	26.9	70.4	39.5	11.0	49.5	$\text{NaBO}_2 \cdot 2\text{H}_2\text{O}$
2.5	9.1	88.4	1.6	6.4	92.0	ice
2.1	33.1	64.8	1.1	56.5	42.4	ice
1.6	33.9	64.5	0.7	38.3	61.0	$\text{NaOH} \cdot \text{H}_2\text{O} + \text{NaOH} \cdot 4\text{H}_2\text{O}$ ( $p5$ )
1.4	9.8	88.8	1.0	6.0	93.0	ice
1.2	33.1	65.7	0.5	35.5	64.0	$\text{NaOH} \cdot 4\text{H}_2\text{O}$
1.1	31.3	67.6	0.3	34.0	65.7	$\text{NaOH} \cdot 4\text{H}_2\text{O}$
0.0	10.1	89.9				ice
0.0	29.3	70.7				$\text{NaOH} \cdot 4\text{H}_2\text{O}$

<sup>a</sup> Compositions and the equilibrium crystalline phases of peritonic points ( $p4$ ,  $p5$ ) and eutonic points ( $e4$ ,  $e5$ ) are underlined.

**Table 4.** Equilibrium Data for the  $\text{KBO}_2 + \text{KOH} + \text{H}_2\text{O}$  System at  $-10^\circ\text{C}^a$

composition of liquid phase (100 w)			composition of wet solid phase (100 w)			equilibrium crystalline phases
$\text{KBO}_2$	$\text{KOH}$	$\text{H}_2\text{O}$	$\text{KBO}_2$	$\text{KOH}$	$\text{H}_2\text{O}$	
30.0	0.0	70.0				$\text{KBO}_2 \cdot 4\text{H}_2\text{O}$
28.7	1.3	70.0	37.4	1.1	61.5	$\text{KBO}_2 \cdot 4\text{H}_2\text{O}$
25.0	4.5	70.5	42.9	1.6	55.5	$\text{KBO}_2 \cdot 4\text{H}_2\text{O}$
24.1	7.2	68.7	41.2	3.7	55.1	$\text{KBO}_2 \cdot 4\text{H}_2\text{O} + \text{KBO}_2 \cdot 1.5\text{H}_2\text{O}$ ( $p6$ )
21.4	10.3	68.3	56.8	3.6	39.6	$\text{KBO}_2 \cdot 1.5\text{H}_2\text{O}$
18.6	0.0	81.4				ice
17.4	7.5	75.1	14.5	5.8	79.7	ice
16.0	16.3	67.7	42.3	8.6	49.1	$\text{KBO}_2 \cdot 1.5\text{H}_2\text{O}$
12.0	22.5	65.5	52.2	8.2	39.6	$\text{KBO}_2 \cdot 1.5\text{H}_2\text{O}$
11.3	11.5	77.2	8.7	8.8	82.5	ice
7.3	29.5	63.2	46.7	12.1	41.2	$\text{KBO}_2 \cdot 1.5\text{H}_2\text{O}$
5.6	32.1	62.3	57.6	8.1	34.3	$\text{KBO}_2 \cdot 1.5\text{H}_2\text{O}$
5.4	14.5	80.1	4.1	11.7	84.2	ice
5.3	38.3	56.4	56.0	10.7	33.3	$\text{KBO}_2 \cdot 1.5\text{H}_2\text{O} + \text{KBO}_2 \cdot 1.25\text{H}_2\text{O}$ ( $p7$ )
4.5	40.1	55.4	52.5	14.4	33.1	$\text{KBO}_2 \cdot 1.25\text{H}_2\text{O}$
4.1	36.1	59.8	42.1	16.2	41.7	$\text{KBO}_2 \cdot 1.5\text{H}_2\text{O}$
3.5	44.3	52.2	41.6	21.9	36.5	$\text{KBO}_2 \cdot 1.25\text{H}_2\text{O}$
3.5	46.5	50.0	15.0	43.7	41.3	$\text{KBO}_2 \cdot 1.25\text{H}_2\text{O} + \text{KOH} \cdot \text{H}_2\text{O}$ ( $e6$ )
1.5	47.3	51.2	1.1	54.3	44.6	$\text{KOH} \cdot \text{H}_2\text{O}$
0.0	47.5	52.5				$\text{KOH} \cdot \text{H}_2\text{O}$
0.0	12.1	87.0				ice

<sup>a</sup> Compositions and the equilibrium crystalline phases of peritonic points ( $p6$ ,  $p7$ ) and eutonic point ( $e6$ ) are underlined.

The solubility diagram of the system  $\text{KBO}_2 + \text{KOH} + \text{H}_2\text{O}$  at  $-10^\circ\text{C}$  (Figure 5, the coordinates of experimental points are given in Table 4) turns out to be no less sophisticated. Crystallization fields of seven solid phases were found in the system, including ice, anhydrous  $\text{KOH}$ , anhydrous  $\text{KBO}_2$ , and the crystalline hydrates  $\text{KBO}_2 \cdot 4\text{H}_2\text{O}$ ,  $\text{KBO}_2 \cdot 1.5\text{H}_2\text{O}$ ,  $\text{KBO}_2 \cdot 1.25\text{H}_2\text{O}$ , and  $\text{KOH} \cdot \text{H}_2\text{O}$ . The  $\text{KBO}_2$  solubility in pure water is  $w = 0.300$  at  $-10^\circ\text{C}$ , which is close to the literature data ( $w = 0.320$ ).<sup>9</sup> At the water vertex, there is an ice crystallization field  $l + \text{ice}$ . On increasing alkali content, metaborate is displaced from the solution, precipitating as, first,  $\text{KBO}_2 \cdot 4\text{H}_2\text{O}$  (the  $l + S_{\text{KBO}_2 \cdot 4\text{H}_2\text{O}}$  field), which loses crystallization water at increasing alkali content, converting into  $\text{KBO}_2 \cdot 1.5\text{H}_2\text{O}$  (the  $l$

+  $S_{\text{KBO}_2 \cdot 1.5\text{H}_2\text{O}}$  field) and, further, into  $\text{KBO}_2 \cdot 1.25\text{H}_2\text{O}$  (the  $l$  +  $S_{\text{KBO}_2 \cdot 1.25\text{H}_2\text{O}}$  field). At KOH introduction into the system, about the same amount of  $\text{KBO}_2$  is removed from the solution, while the crystalline phase composition changes. Then the total solubility rapidly grows owing to KOH, reaching its maximum at the eutonic point  $e_6$ . The points  $p_6$  and  $p_7$  are associated with the peritonic transitions  $\text{KBO}_2 \cdot 4\text{H}_2\text{O} \leftrightarrow \text{KBO}_2 \cdot 1.5\text{H}_2\text{O}$  and  $\text{KBO}_2 \cdot 1.5\text{H}_2\text{O} \leftrightarrow \text{KBO}_2 \cdot 1.25\text{H}_2\text{O}$ , respectively. The bottom part of the diagram corresponds to a mixture of solid components.

Analyzing the solubility in the four ternary systems under study, the opposite influence of the alkali cation nature has been observed. Indeed, in the borohydride ternary systems, the sodium salt has the best solubility, while the corresponding potassium salt is much less soluble. Sodium borohydride dissolves well both in pure water (0.234 of  $\text{NaBH}_4$  against 0.113 of  $\text{KBH}_4$  at  $-10^\circ\text{C}$ ) and in strongly alkaline solutions: a solution containing 0.105 of  $\text{NaBH}_4$  and 0.426 of  $\text{NaOH}$  is in equilibrium with the precipitate at the eutonic point  $e_1$ ! On the contrary, potassium borohydride is almost insoluble in water–alkali mixtures even at relatively low KOH concentrations.

In the borate systems the situation is the opposite. Potassium metaborate forms a highly concentrated aqueous solution at  $-10^\circ\text{C}$ , whereas sodium metaborate is generally insoluble (it forms a solid mixture with ice). Introducing a sufficient amount of  $\text{NaOH}$  into the system results in transferring part of sodium metaborate to the solution; nevertheless, at all ratios the  $\text{NaBO}_2$  concentration in the saturated solution is within  $w = (0.027 \text{ to } 0.051)$  only.  $\text{KBO}_2$  is much more soluble; its concentration at an increasing alkalinity gradually decreases from  $w = 0.300$  in pure water down to  $w = 0.035$  at the eutonic point  $e_6$ . Thus, the  $\text{KBO}_2$  solubility remains above  $w \approx 0.1$  in the practically important concentration range. The phase diagrams of the  $\text{NaBH}_4 + \text{NaOH} + \text{H}_2\text{O}$  and  $\text{KOH} + \text{KBO}_2 + \text{H}_2\text{O}$  systems have the largest area of the homogeneous-liquid state  $l$ , and the  $\text{KBH}_4 + \text{KOH} + \text{H}_2\text{O}$  and  $\text{NaOH} + \text{NaBO}_2 + \text{H}_2\text{O}$  systems have the least.

Thus, according to our study, the systems with sodium and potassium ions considerably differ by the solubility of both the initial fuel components and the products of FC discharge. These data have essential importance for the development of FCs with the borohydride fuel. The high concentration of the borohydride ion  $\text{BH}_4^-$  in solution is extremely important from the viewpoint of electrochemistry, kinetics, and power engineering of borohydride utilization in a FC. The high solubility of the  $\text{BO}_2^-$  ion is significant from the viewpoint of avoiding accumulation of the discharge products in the porous structure of FC electrodes. The optimum choice of the components ratio is possible by means of joint use of our phase diagrams.

## Conclusions

A critical analysis of the scientific literature shows that there are many reports on studies of the aqueous solubility of  $\text{NaOH}$ ,  $\text{NaBO}_2$ ,  $\text{NaBH}_4$ ,  $\text{KOH}$ ,  $\text{KBH}_4$ , and  $\text{KBO}_2$  both individually and in various double mixtures. However, from a fundamental and practical point of view, of greater interest are ternary systems in which the solubility of the components can strongly differ from the individual solubility of each component. The ternary systems  $\text{NaBH}_4\text{--NaOH--H}_2\text{O}$ ,  $\text{KBH}_4\text{--KOH--H}_2\text{O}$ ,  $\text{NaOH--NaBO}_2\text{--H}_2\text{O}$ , and  $\text{KOH--KBO}_2\text{--H}_2\text{O}$  are of special interest. Mixtures belonging to the first two systems are used as a fuel and as a hydrogen source in hydrogen power engineering, including low-temperature FCs. In the course of their oxidation, borohydrides are converted into metaborates. Hence, mixtures

belonging to the last two systems represent the discharged product of hydrogen power engineering. The performance of such mixtures is determined by the solubility of their components, negative temperatures being especially critical. Therefore, in the present work we investigated the aforementioned ternary systems at  $-10^\circ\text{C}$ . The compositions of the equilibrium liquid and solid phases and the compositions of the eutonic and peritonic equilibria have been determined for all four systems by the method of isothermal saturation. The coordinates of the homogeneous solution ranges in the solubility diagrams have been defined for all four systems as well. The best solubility of the solid components at  $-10^\circ\text{C}$  is characteristic of the systems  $\text{NaBH}_4\text{--NaOH--H}_2\text{O}$  and  $\text{KOH--KBO}_2\text{--H}_2\text{O}$ .

## Acknowledgment

The authors are grateful to Prof. K. K. Il'in for valuable advice and Prof. A. A. Kamnev for improving the English.

## Literature Cited

- (1) Kim, Ch.; Kim, K. J.; Ha, M. Y. Investigation of the characteristics of a stacked direct borohydride fuel cell for portable applications. *J. Power Sources* **2008**, *180*, 114–121.
- (2) Liu, B. H.; Li, Z. P. Current status and progress of direct borohydride fuel cell technology development. *J. Power Sources* **2009**, *187*, 291–297.
- (3) Liu, B. H.; Li, Z. P.; Arai, K.; Suda, S. Performance improvement of a micro borohydride fuel cell operating at ambient conditions. *Electrochim. Acta* **2005**, *50*, 3719–3725.
- (4) Churikov, A. V.; Ivanishchev, A. V.; Zapsis, K. V.; Sycheva, V. O.; Gamayunova, I. M. Fuel cells using borohydride fuel. *Russ. J. Power Sources* **2009**, *9*, 117–127.
- (5) Nikolskiy, B. P.; Grigorov, O. N.; Pozin, M. E. *Chemist's Handbook*, Vol. 1; Khimiya Press: Leningrad, 1971.
- (6) Mikheeva, V. I.; Breystis, V. B. Polyterm of solubility of the system  $\text{NaBH}_4\text{--H}_2\text{O}$  and isotherm of solubility of the system  $\text{NaBH}_4\text{--NaOH--H}_2\text{O}$  at 0, 18, 30 and  $50^\circ\text{C}$ . *Russ. J. Inorg. Chem.* **1960**, *5*, 2553–2563.
- (7) Mikheeva, V. I.; Selivokhina, M. C. Solubility in systems  $\text{KBH}_4\text{--H}_2\text{O}$  and  $\text{KBH}_4\text{--KOH--H}_2\text{O}$ . *Rus. J. Inorg. Chem.* **1963**, *8*, 439–446.
- (8) Toledano, P.; Benhassaine, A. Studying of system sodium metaborate–water on the device of a differential thermal analysis under pressure. *C. R. Acad. Sci.* **1970**, *271*, 1577–1580.
- (9) Skvorstov, V. G.; Druzhinin, I. G. Polyterm of solubility of the binary systems  $\text{H}_3\text{BO}_3\text{--H}_2\text{O}$ ,  $\text{KBO}_2\text{--H}_2\text{O}$  and the diagram of fusibility  $\text{CO}(\text{NH}_2)_2\text{--H}_3\text{BO}_3$ . *Uch. Zap., Chuv. Gos. Pedagog. Inst.* **1969**, *29*, 150–163.
- (10) Toledano, P. Equilibrium liquid–solid body in a binary system water–potassium metaborate. *C. R. Acad. Sci.* **1962**, *254*, 2348–2350.
- (11) Babayan, G. G.; Oganeyan, E. B.; Gyunashyan, A. P.; Sayamyan, E. A. The diagram of solubility of the system  $\text{NaOH--KOH--H}_2\text{O}$  at 0 and  $20^\circ\text{C}$ . *Izv. Akad. Nauk Arm. SSR, Ser. Khim.* **1963**, *16*, 539–545.
- (12) Mikheeva, V. I.; Breystis, V. B. Isotherm of solubility of the sodium borohydride and sodium hydrate in water at  $0^\circ\text{C}$ . *Dokl. Akad. Nauk SSSR* **1960**, *131*, 1349–1350.
- (13) Lukyanova, E. N.; Kokhova, V. F. Isotherm of solubility in the system  $\text{NaOH--NaBH}_4\text{--NaCl--H}_2\text{O}$  at  $25^\circ\text{C}$ . *Russ. J. Inorg. Chem.* **1963**, *8*, 218–225.
- (14) Frontasyev, V. P.; Sakharova, Yu. G.; Sakharova, N. N. Water solubility of complexes acetates of the lanthanum, cerium, praseodymium, neodymium and samarium with thiourea. *Russ. J. Inorg. Chem.* **1965**, *10*, 1816–1821.
- (15) Dymova, T. N.; Eliseeva, H. G.; Mikheeva, V. I. Thermographic study of the sodium borohydride and some related substances. *Russ. J. Inorg. Chem.* **1967**, *12*, 2317–2320.
- (16) Mikheeva, V. I.; Breystis, V. B.; Kuznestov, V. A.; Kryukova, O. N. Reaction sodium borohydride with sodium hydroxide. *Dokl. Akad. Nauk SSSR* **1969**, *187*, 103–105.
- (17) Mikheeva, V. I.; Kuznestov, V. A. Stoichiometry of reaction sodium borohydride with hydroxide. *Russ. J. Inorg. Chem.* **1971**, *16*, 1212–1217.

Received for review May 28, 2010. Accepted December 3, 2010. The authors are grateful to the Federal Education Agency of the Russian Federation for financial support (Contract #P183).